Subpixel sensitivity map for a charge-coupled device sensor

Daniel Kavaldjiev, MEMBER SPIE
Zoran Ninkov, MEMBER SPIE
Rochester Institute of Technology
Center for Imaging Science
54 Lomb Memorial Drive
Rochester, New York 14623
E-mail: dik4399@cis.rit.edu

Abstract. The sensitivity across a solid state detector array varies as a result of differences in transmission, diffusion and scattering properties over the sensor. This variation will occur over a range of scale lengths and its knowledge is of importance for improved device design and in a variety of applications, for example, event centroiding in photon counting systems. A measurement of the sensitivity variation on a subpixel scale for a two-phase front-illuminated CCD is reported. The measurement is made using a scanning reflection microscope. A variation in sensitivity between the phases within a pixel is clearly observed, as well as variations on a much smaller spatial scale. [S0091-3286(98)03103-1]

Subject terms: charge-coupled device; pixel sensitivity; response function; crosstalk.

Paper 20057 received May 20, 1997; revised manuscript received Oct. 2, 1997; accepted for publication Oct. 2, 1997.

1 Introduction

It is well known that the sensitivity of a solid state imager will exhibit spatial variations that influence the point spread function of the imager. This variation, in the case of front-illuminated CCDs, is due to transmittance nonuniformity, quantum efficiency spatial variations, diffusion spreading of the photogenerated minority carriers, optical crosstalk, spatial quantization and transfer inefficiency, among other effects. Theoretical calculations have been attempted to model these effects.[1–8] Experimental measurements have also been previously reported,[9–11] but with resolution of the order of several times the wavelength of light used.

The spatial response of any shift-invariant detector can be equivalently described either in the space domain, through its point spread function (PSF), or in the spatial frequency domain, by its modulation transfer function (MTF). Any discrete array of photoelements, such as a CCD, will perform sampling of the input image, destroying the conditions for shift-invariance and making the MTF concept if not questionable, at least one in need of further redefinition.[12–15] Moreover, MTF measurements detect the modulus of the PSF Fourier transform, and the loss of phase information prevents a correct PSF reconstruction in the case of asymmetrical form of the detector PSF. Therefore in this paper, a more physically meaningful path was selected, namely characterization of the detector with its PSF. The knowledge of this function is of importance for improved device design and in applications such as event centroiding in photon counting systems[16] and accurate photometry.[17,18]

This paper reports on the measurement of sensitivity variation on a subpixel scale for a two-phase front-illuminated CCD. These measurements were made with a resolution close to the diffraction limit, achieved using a scanning reflection microscope. An optical spot of size between 0.4 and 0.5 μm (depending on the wavelength of the light used) was scanned in a stepped raster fashion over a single pixel and its immediate neighbors. The CCD was read out at each point of the scan. The signal from the partially illuminated pixel as a function of the spot position provides a map of the spatial pixel sensitivity, while the signal detected by the neighboring pixels is a measure of the pixel crosstalk. The reflection image of the CCD was also obtained and used to locate the position of the optical spot absolutely.

Section 2 describes the theoretical formulation of the experiment, Section 3 describes the setup and the experimental procedure used, and Section 4 presents the experimental results, which are then discussed in Section 5.

2 Theoretical Formulation

If an optical spot of size smaller than the pixel dimension is scanned over the detector, the output signal is in the form $R(n,m;x,y)$, giving the response of pixel (n,m) when the center of the light spot is at (x,y), as shown in Figure 1. If the PSF of the optics is PSF_0, the response is given by:

$$R(n,m;x,y)=\mathrm{PSF}_0(x,y)\otimes R'(n,m;x,y), \tag{1}$$

where R' is the response in the case of illumination by a δ-function (point) light source, and can be thought of as a 4-D PSF for the detector. Since R' depends explicitly on the input coordinates (x,y), the system is shift-variant. Two cases can be considered:

- In one case, (x,y) are coordinates within pixel (n,m): R' then represents a map of the *spatial pixel sensitivity*, i.e., the response of the pixel as a function of the position of the source on it.
- In the other case, (x,y) are coordinates outside pixel (n,m) boundaries. In this case, R' is a measure of the

 0091-3286/98/$10.00

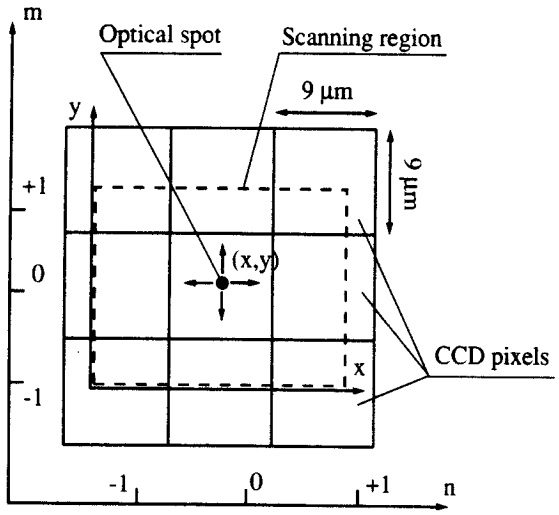

Fig. 1 Geometry of the generalized experiment. The solid squares represent a 3×3 CCD pixel subarray. The optical spot (dark filled circle) is scanned over the array in a raster fashion within the scanning region (dashed line rectangle).

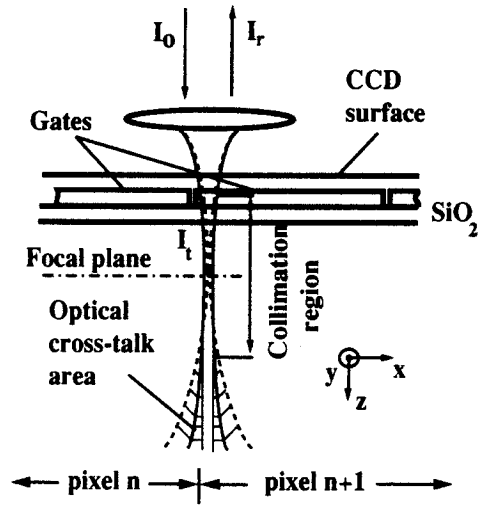

Fig. 2 Cross section of the illumination spot geometry used in this experiment. The light intensity distribution in the bulk is shown for two different numerical apertures. The higher NA is shown with the dashed line. The smaller NA (solid lines) corresponds to that used in the experiment described in this paper.

cross-pixel response, i.e., the response of the pixel as a function of the position of the source on a neighboring pixel.

As a PSF, R' *completely* defines the imaging characteristics of the CCD. It includes any variations attributable to transmission, diffusion, aperture and transfer inefficiency factors, as well as the effect of read-out electronics (quantization errors etc.).

If this function R' is to be measured directly, a spatial δ-source must be used. In reality, an illuminating source is needed with the smallest possible spatial dimensions on the CCD to keep photogeneration as localized as possible. The problem is analogous to selecting an optical microscope with the highest spatial resolution. Initially it was thought that a near-field scanning optical microscope[19] (NSOM) would be employed. The NSOM consists of an aperture several times smaller than the wavelength of the optical radiation commonly located at the sharp end of a tapered optic fiber tip or a micropipette that has a thin metallic coating applied. This aperture is placed in close proximity to the sample and is used to illuminate the sample in the near field. The size of the illuminating spot with this techniques can be as small as $\lambda/20$, where λ is the wavelength of the incident light. This size is directly determined by (1) the size of the scanning aperture and (2) by its distance to the sample, typically 1 to 10 nm. In the present case, the "sample," i.e., the CCD active region, is located below the $Si:SiO_2$ interface, and therefore the minimum aperture sample separation is of the order of a micrometer. This large sample separation results in the NSOM optical spot being larger than the one that can be obtained using a conventional far-field microscope. In addition, the intensity distribution divergence in the NSOM case is greater than in the far-field configuration, increasing the optical crosstalk (see later) to unacceptable levels. Therefore, NSOM is not applicable *in principle* for the present purpose.

Another possibility was to use a high numerical aperture (NA) objective in a conventional scanning microscope configuration. Such a microscope exhibits spatial resolution $\sim\lambda/2NA$. For an air-spaced objective-sample separation, or dry system, $NA \leq 1$, with a minimum achievable spot size $\sim\lambda/2$. If an immersion oil were applied to the surface of the CCD (without damaging it), an oil-immersion objective with NA as high as 1.5 can be used, giving a lateral resolution for $\lambda = 488$ nm (blue line of Ar^+ laser) of the order of 0.2 μm. This is the highest lateral resolution that could be achieved with conventional optical microscopy. However, an oil-immersion microscope may not be desirable when the sample is a CCD for a number of reasons, discussed below.

First, using a higher NA will result in an increased *optical crosstalk*. Any carriers, detected in a pixel that is not the illuminated pixel, are referred to as a crosstalk. Diffusion crosstalk is a result of carriers generated in the illuminated pixel, diffusing within the semiconductor and being collected by a neighboring pixel. Optical crosstalk, on the other hand, is a result of carriers being produced in a neighboring pixel because photons slightly illuminate that pixel even when the interrogating optical spot is not centered on it. This is the case for instance when an optical source of finite dimensions is positioned very close to the periphery of a pixel, and 2 pixels are illuminated simultaneously. If the "illuminated" pixel is defined to be the one containing the center of the stimulating spot, part of the signal detected by the neighboring pixel is then a result of the optical crosstalk. An increase in the objective NA results in an increase in the optical crosstalk as a results of an increased divergence of the light intensity distribution in the bulk of the semiconductor (shown in Figure 2, dashed lines). Because of this increased optical footprint in the bulk, when the center of the illuminating spot is close to the pixel boundary, the neighboring pixel will detect carriers generated within its volume, even though the surface spot appears to be contained within a single pixel. This optical crosstalk therefore comes from the experimental setup rather than being a property of the detector itself (and is

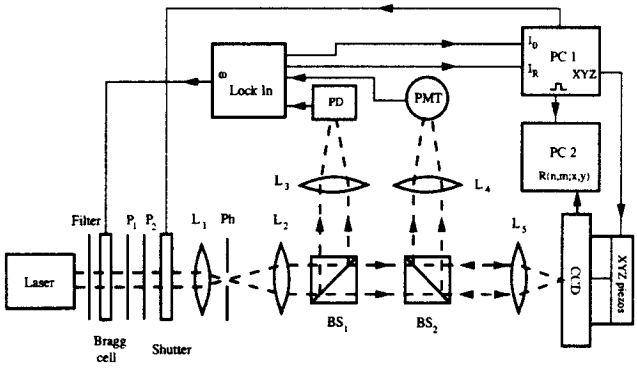

Fig. 3 Experimental setup for measurement of the subpixel sensitivity function of a CCD detector: P_1 and P_2 are polarizers used for light intensity control; L_5 is the imaging objective; PMT is a photomultiplier tube used to obtain the reflection image of the CCD surface; PD is the photodiode, monitoring the incident light intensity; PC_1 and PC_2 are two computers for data collection and control.

different from diffusion crosstalk), and represents an experimental limitation that must be minimized.

Second, the refractive index of the immersion oil is very close to that of the glass, and applying it to the surface of the CCD drastically changes the Maxwell boundary conditions at the air-surface interface. This would lead to significantly different transmission and reflection coefficients. Since transmission variations play a dominant role in the spatial variation of pixel sensitivity, the use of oil would alter the irradiance arriving in the active region of the detector and therefore the detected PSF would differ from that found in normal operation. On the other hand, such a technique would enable decoupling, to a certain degree, of the transmission and collection efficiency effects, and direct measurement of the latter.

For the purpose of this work, an air-spaced microscope configuration was adopted. The factors influencing the spatial variation of the CCD subpixel sensitivity were suspected to be wavelength-dependent. To "bracket" the results for the two ends of the visible spectrum, the scanning microscope experiment was performed at two different wavelengths—488 nm using an argon ion laser, and 633 nm using a HeNe laser.

3 Experimental Setup

The experimental procedure follows the general idea outlined earlier. A laser beam was focused on the CCD in the form of a spot of size $\sim 0.4\ \mu m$ for $\lambda = 488$ nm and $\sim 0.5\ \mu m$ for $\lambda = 633$ nm. This spot is scanned in a stepped raster fashion over a single pixel and its immediate neighbors, and at each position the CCD was read out. From this set of images, the pixel sensitivity and the crosstalk can be derived. In addition, a reflection image of the surface was obtained to enable an estimate of the correlation between the surface structure and sensitivity map.

The experimental setup is shown in Figure 3. It is essentially a scanning reflecting microscope with the CCD as the sample. The optical system consists of two parts. The illumination part includes filter F; polarizers P_1 and P_2; objectives L_1, L_2, L_3, and L_5; and pinhole Ph. The reflection collection part includes objectives L_5 and L_4. Light intensity is controlled by a pair of polarizers P_1 and P_2 and the mechanical shutter. Spatial beam cleaning is performed by an objective L_1 (NA = 0.85), pinhole Ph (5 μm) and objective L_2 (NA = 0.25). The beam intensity through the remainder of the system can be considered spatially uniform. The light is focused on the surface of the CCD by the imaging objective L_5 (NA = 0.6). The photomultiplier (PMT) records the reflection image from the CCD surface, $I_r(x,y)$, which is used to locate the optical spot position absolutely.

The size of the photogeneration source is defined by the focal intensity distribution of the imaging objective L_5. It is crucial for the validity of the results that this distribution is identical at every scanned position on the CCD. To ensure this, scanning was performed by moving the CCD, thereby maintaining an axially aligned stationary optical system. The imaging objective used is highly corrected for spherical abberation (Olympus MS LWD Plan 40x, NA = 0.6), so the focal distribution can be considered diffraction limited. In the focal plane, the radial distribution is given by the Airy function. Along the optical axis the extension of the region of "collimation" around the focal plane (depth of field for the experiment) is[20] around 1.5 μm for $\lambda = 488$ nm. The absorption length of light in Si at this wavelength is[5] $\approx 1\ \mu m$, so to a first approximation, the photogeneration source can be considered as an axially uniform beam with Airy function intensity radial distribution, i.e., cylindrical photogeneration source (see Figure 2). For red light with $\lambda = 633$ nm the collimation region is of the order of 2 μm, the absorption length is $\sim 2.3\ \mu m$, so the experimental geometry remains unchanged.

The CCD head is mounted on an XYZ stage of three piezoelectric translators, whose position was controlled by a computer PC1. The Z direction is along the optical axis, while the scanning was performed in XY directions. The CCD used was an Eastman Kodak model KAF4200 two-phase device, consisting of 2033×2044 pixels, each $9 \times 9\ \mu m$ in area. The CCD readout was performed by a computer PC2, using a Photometrics CE200 camera electronics controller equipped with a 12 bit/500 kHz analog-to-digital (A/D) board.

There are number of sources of noise with this experimental arrangement including laser power fluctuations, sensor noise, and noise from mechanical drift of the piezo stages. The last of these, drift, was estimated from repeated reflection scans of the array to be around 0.5 μm/hour. As the total drift needed to be kept smaller than the lateral resolution of the microscope (0.5 μm), the total scanning time was necessarily limited to less than 1 hour. The effect of the laser noise was reduced by increasing integration time at each spot position and thereby averaging over such fluctuations.

The spatial dimension of the CCD scanned region was determined by the scanning time available and the desired resolution, and was required to encompass at least an entire pixel with parts of its nearest neighbors. As a result of the preceding considerations, and taking into account various software and hardware speed limitations, the shutter speed was selected to be 200 ms (i.e., the integration time for

each spot), and the scanning range 15 to 20 μm with 50 $\times$ 50 scan points.

Ideally, the reflectance and the CCD-detected image should be obtained simultaneously. However, the saturation signal of KAF 4200 is $\approx$80,000 e^-, or $\sim 7\times10^{-14}$ J for $\lambda = 550$ nm photons (average wavelength). Using a CCD quantum efficiency of 40% (from the Kodak data specification sheet) and an integrating time of 200 ms, the full well incident energy translates into a maximum of incident optical power of 0.3 pW. At the first air-silicon oxide interface the reflectivity would be of the order of a few percent. Therefore the reflected signal from the CCD would be less than 20 fW. The SNR, obtained for this reflection signal using the photomultiplier, is much less than unity, and thus the signal would be undetectable. Therefore the reflection image had to be taken in a separate scan with a higher illumination level than that used to obtain the CCD sensitivity image.

The experimental procedure adopted was to gather date in three consecutive scans of the optical spot over the CCD. At the beginning of the experiment, the spot was positioned at the origin of the scanning region. The spot was scanned over the desired region, and the reflectance image $I_r(x,y)$ of the CCD recorded (i.e., readout). The optical spot was then moved back to the origin, presumably to the *same* position as used at the beginning of the reflectance scanning. The spot was scanned again over the same region as before, but this time at every position of the scan the image of the spot as detected by the CCD was recorded. From this set of CCD images (one for every position) the function $R(n,m;x,y)$ was reconstructed, and was a measure of the PSF of the detector. From $R(n,m;x,y)$ the pixel sensitivity, the crosstalk, and MTF can be derived. At the end of this second scan, the spot was moved back to the origin position and another reflection scan was performed. The two reflection images (before and after the sensitivity map measurement) were compared, and if they were identical the experimental data was acceptable. Otherwise the data was discarded, since any discrepancy between the two images suggested drift in the piezo stages over the time scale of the experiment.

The laser light intensity $I_0(x,y)$ was monitored during the experiment by photodiode (PD). The reflectance signal from the CCD, $I_r(x,y)$ and the measured CCD signal $R(n,m;x,y)$ are normalized using $I_0(x,y)$ at every position of the scan, so the noise attributable to the intensity variations in the light source were minimized. The total noise was estimated to be of the order of 0.2% of the full well signal.

4 Results

The results from the described experiment are shown in Figure 4 for $\lambda = 488$ nm and Figure 5 for $\lambda = 633$ nm.

Reflection images are shown in Figures 4(a) and 5(a). The boundaries of the central pixel are marked by the dashed line. The direction of the charge transfer is in the negative X axis. The two phases of the CCD are clearly seen as difference in the reflected signal over the two halves of the pixel. This pixel shown corresponds to pixel (0,0) in Figure 1 and is referred to henceforth as the *pixel of interest* (POI). The normalized signal detected by the POI

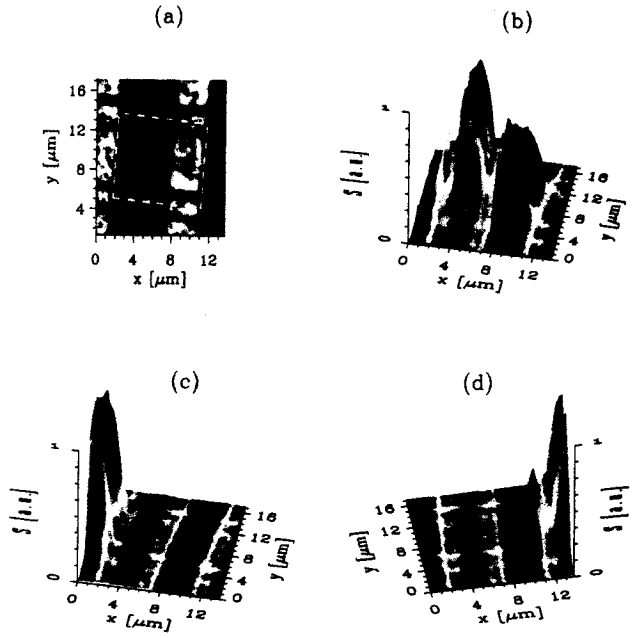

Fig. 4 Experimental data for 488 nm wavelength: (a) reflection image of the CCD surface, where the boundaries of pixel (0,0) are shown; (b) signal S detected by pixel (0,0), as a function of the optical spot position, the grayscale shading is the pseudotransmission; (c) signal detected by pixel $(-1,0)$; and (d) signal detected by pixel (1,0).

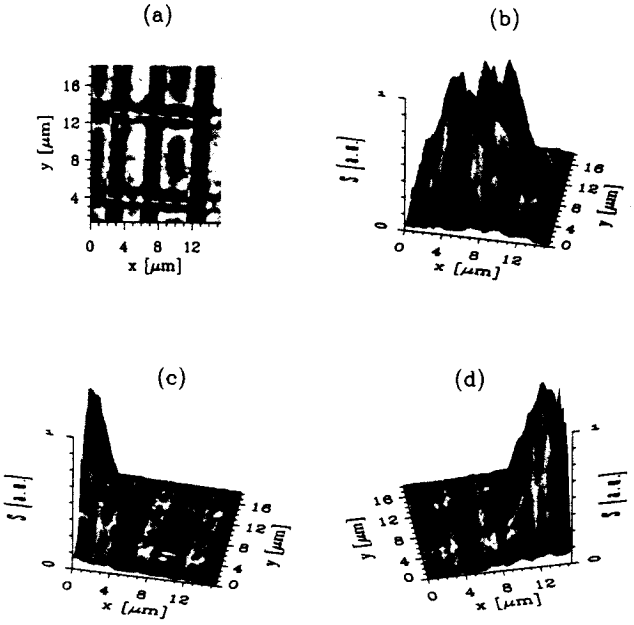

Fig. 5 Experimental data for 633 nm wavelength: (a) reflection image of the CCD surface, where the boundaries of pixel (0,0) are shown; (b) signal S detected by pixel (0,0), as a function of the optical spot position, the grayscale shading is the pseudotransmission; (c) signal detected by pixel $(-1,0)$; and (d) signal detected by pixel (1,0).

as a function of the spot position, is shown as the height of the surface in Figures 4(b) and 5(b). In Figures 4(b), 4(c), 5(b), and 5(c), the signal detected by the pixel $(-1,0)$ (the pixel to the left of the POI) and pixel $(+1,0)$ (the pixel to

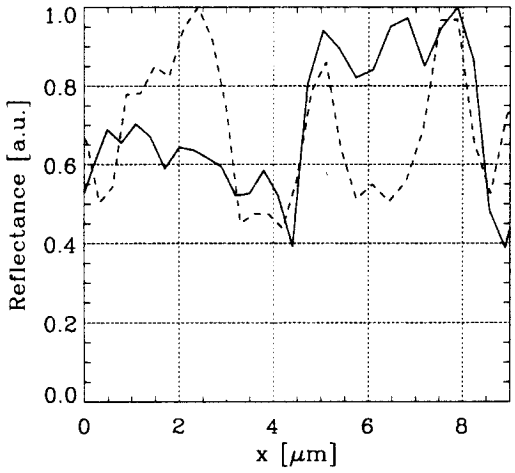

Fig. 6 Reflectance line scans in the x-direction through the POI, for an illumination at 488 nm (solid line) and 633 nm (dashed line). Note the reversal of the ratio of the relative reflectances between the two wavelengths at $x=2$ μm and $x=6$ μm.

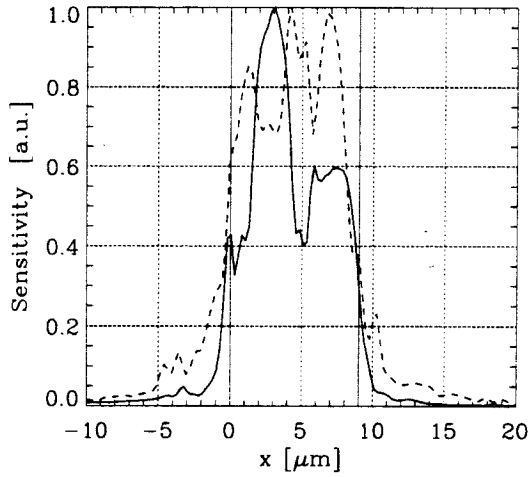

Fig. 7 Sensitivity line scans in the x-direction through the POI (averaged in the y-direction over several scans), for an illumination at 488 nm (solid line) and 633 nm (dashed line). The solid vertical lines at $x=0$ μm and $x=9$ μm mark the pixel extent.

the right of the POI) are shown. The grayscale shade of the surface shown is a complimentary of the reflection image (its values are calculated as a constant value minus the reflection image values), and is referred to as the *pseudotransmission*. To calculate the actual absolute transmission, the absorption of the layers above the Si active region must have been known, and the reflectance measurements must have been made using an integrating sphere to eliminate the effects of surface scattering or oblique reflection. This estimate of the transmission (the pseudotransmission) assumes constant absorption in the overlaying gate structure, and serves as a first-order estimate of the amount of light reaching the CCD's active region.

The close general correspondence between the pseudotransmission and the sensitivity can be seen in Figures 4(b) and 5(b). The low pseudotransmission (dark) regions are seen to coincide, in general, with low sensitivity (i.e., low height) regions. The greatest sensitivity variation within the pixel is seen to be between the two phases of the CCD, attributable to different transmissivities and/or charge collection efficiencies. Strictly speaking, unless the absorption in the overlaying regions is known, it cannot be inferred from these results which of these two effects is dominant. However, comparison between the results obtained at the two wavelengths provides additional information. In the reflectance images, the ratio of the phase reflectivities can be seen to be reversed between the two experimental wavelengths. This can be seen in Figures 4(a) and 5(a), and is also evident in Figure 6, where reflectance line scans in the x-direction through the center of the POI are shown for the two wavelengths. The phase that is darker at 488 nm (phase 2 in Figure 6), is brighter at 633 nm (phase 1 in Figure 6). This implies that interferometric effects are primarily responsible for the reflectivity and therefore also for the transmission variations. The collection efficiency, on the other hand, has a monotonic wavelength dependence (due to monotonic wavelength dependence of the absorption depth), and if these effects were dominant, the sensitivity ratio between the two phases would be either greater or less than unity at both wavelengths. The sensitivity ratio is reversed between the two wavelengths, as can be seen by inspection of Figures 4(b) and 5(b). It is also evident in Figure 7, where sensitivity line scans in the x-direction (averaged in the y-direction over several scan lines) are shown for the two illumination wavelengths. Because of the sensitivity ratio reversal, the dominant cause of the sensitivity difference between the pixel phases must be due to transmission variations.[9]

In addition, microvariations of the pixel sensitivity on a scale of about 1 μm are also observed in Figures 4 and 5. These are probably the result of gate polysilicon nonuniformities, as caused by local variations of the polysilicon thickness and grain formation. Such nonuniformity would create localized changes in the thin-film reflectivity and absorption, resulting in transmission variations, and, in turn, to sensitivity variations.

Several scans were performed centered on different POIs on the CCD array to observe if there were differences in the subpixel spatial sensitivity maps for different pixels. An example of such maps, measured at 633 nm, for two different pixels is shown in Figure 8 [Figure 8(a) corresponds to the same pixel as in Figure 5(c)]. The overall form of the sensitivity map (the two-phase structure) is very similar for the different pixels. Differences are, however, observed in the small scale structure within the pixel.

5 Discussion

The cross-pixel response, or crosstalk between pixels, manifests itself as a nonzero signal in the POI when the optical spot is located outside the boundaries of the POI. This is easily seen in Figures 4(c), 4(d), 5(c), and 5(d), which show the signal detected by the pixels above and below the POI in a column of the CCD.

The crosstalk has a spatial extent beyond the boundaries of the scanning region [nonzero signal along the edges of Figures 4(c), 5(c) and 8]. The extent of the scanning region was restricted by the experimental conditions, as explained in Section 3, and included the entire POI area but only parts of the eight neighboring CCD pixels. The form of the crosstalk is observed not to vary significantly for different

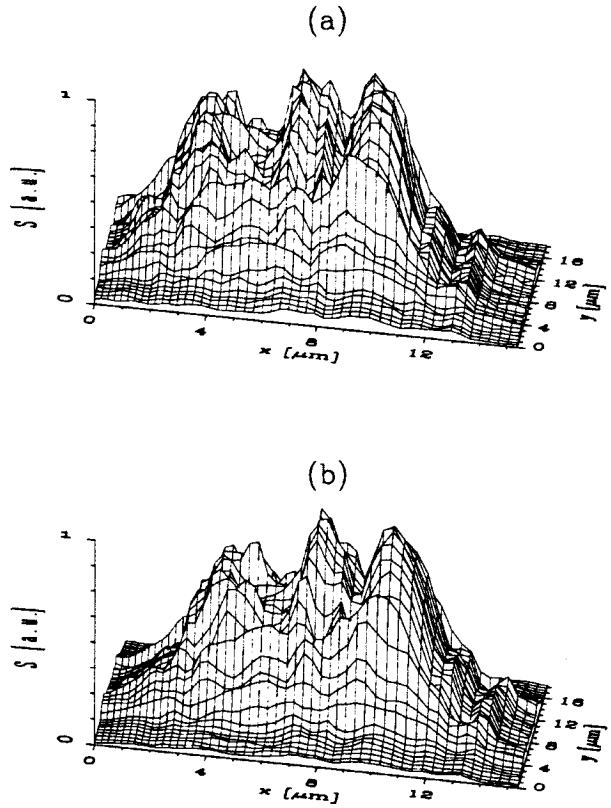

Fig. 8 Sensitivity S measured using 633 nm wavelength source for two different CCD pixels (330,612 and 325,705). Data shown in (a) is from the same pixel shown in Figure 5. Large scale variations are the same, but smaller scale variations differ.

POIs (see Figure 8), i.e., the crosstalk detected by the POI when the optical spot was within pixel $(-1,0)$, is the same as the signal detected by pixel (1,0) when the spot was over the POI. This allows for the "expansion" of the scanning region by padding the crosstalk data from the neighboring pixels. The total pixel sensitivity functions, combined in this manner, are shown in Figures 9(a) and 9(b) for illumination by blue and red light, respectively. The height of the surfaces in Figure 9 are again the measured signal. For every scan position of the optical spot, the CCD pixel with the maximum detected signal was identified. The spot was then assigned to have been located "within" this pixel. In this way, the boundaries of the pixels were determined and are shown by the different graylevels in Figure 9. As can be seen, the pixel boundaries shown are not exact straight lines due to discretization errors in optical spot position. The boundaries are not sharp due to graylevel interpolation, performed by the plotting software.

The crosstalk between columns (y-direction) in Figure 9 is significantly less than the crosstalk in the direction of the charge transfer along the columns (negative x-direction) as a result of the presence of a channel stop. As has already been discussed, the optical crosstalk, arising from the finite source size and the axial variation of the intensity distribution (see Section 2) will be coupled with that resulting from diffusion. An analysis of this experimental data shows however that the effect observed here is principally diffusion crosstalk. This is deduced because (1) the extent of the optical crosstalk is only $\sim 0.5\ \mu$m, whereas the extent of

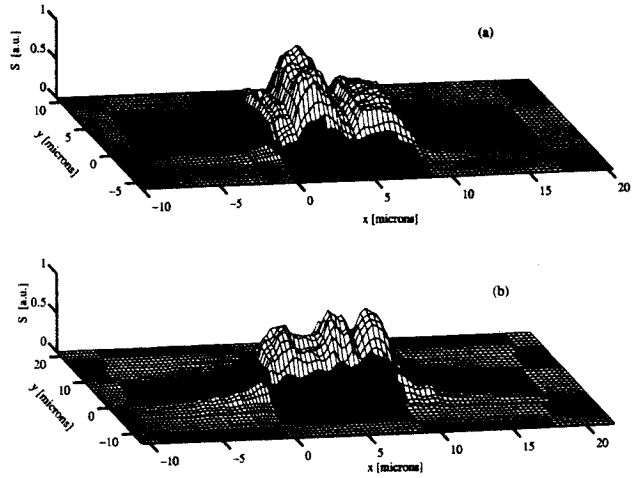

Fig. 9 Pixel sensitivity functions. Different graylevels corresponds to different pixel areas: (a) 488 nm incident light and (b) 633 nm incident light. The sensitivity function in (b) is shown over a larger extent in the y-direction to include the increased crosstalk between columns for an illumination at 633 nm.

the observed crosstalk is 2 to 4 μm depending on the wavelength; and (2) the observed crosstalk is spatially asymmetric (note the crosstalk extent in x-direction in Figures 6 and 9), while that expected from the optical crosstalk would be symmetric. To convincingly prove that the observed asymmetry of the sensitivity function in the charge transfer direction is a real CCD detector property, and not a result of an asymmetry in the incident light intensity distribution, the experiment was repeated with the CCD rotated by 90 and 180 deg. The measured sensitivity functions were found to be independent of the CCD orientation.

The presence of such asymmetry in the detector response can only be found by measurements in the spatial domain, as presented in this paper. Measurements in the frequency domain, such as MTF and contrast-transfer function (CTF) measurements, detect only the modulus of the Fourier transform. The loss of the phase information in the Fourier domain distorts the calculated PSF, especially through the loss of the asymmetry information. Therefore, MTF (or CTF) experimental characterization of solid state detectors, although less time consuming and far simpler in experimental setup, severely limits the amount of extracted information about device performance.

The observed deviation of the pixel sensitivity function from a symmetrical form has implications in a variety of areas. One example would be in pixel centroiding algorithms, designed for determining, with subpixel accuracy, the center of a light distribution falling on the detector. Such requirements are encountered in astronomy, machine vision and spectrometry.[21,22] Quantitative estimates of the influence of the actual measured PSF of the CCD detector (using the results presented here) on the accuracy of the various centroiding algorithms is currently under investigation and will be a subject of a future paper.

Another notable feature seen in the sensitivity function is the dramatically increased crosstalk along the channel stops, most probably due to local minima in the potential distribution, forming channels through which the minority carriers can diffuse to the nearest pixel. Some crosstalk is

also present close to the edge of the phase gates, probably the result of potential effects along the phase dopings. These crosstalk effects are more pronounced at the longer wavelength, as would be expected[5] because of the larger absorption length in Si.

6 Conclusions

The spatial pixel sensitivity and the pixel crosstalk of a front-illuminated CCD detector was measured with resolution close to the theoretical maximum for the two wavelengths in the visible spectrum. Micro and macrovariations of the sensitivity within a pixel were observed. The macrovariations appear closely related to transmission variations. Increased crosstalk along channel stops and phase dopings was also measured. The variations of the pixel sensitivity from a constant value over the entire pixel will have implications in the areas of device design and in imaging applications such as event centroiding in photon counting systems.

Acknowledgments

This work was supported in part by funding from the National Science Foundation, the S/IUCRC program, and the New York State CAT program. We would like to acknowledge the help of our colleagues, namely Mehdi Vaez-Iravani, now of KLA-Tencor, Gerry Lubberts of the Rochester Institute of Technology and Bruce Burkey at Eastman Kodak.

References

1. D. H. Seib, "Carrier diffusion degradation of MTF in CCD," *IEEE Trans. Electron. Dev.* **ED-21**(3), 210–217 (1974).
2. M. M. Blouke, "A method for improving the spatial resolution of illuminated CCD's," *IEEE Trans. Electron. Dev.* **ED-28**(3), 251–256 (1981).
3. W. Buchtemann, "MTF of extrinsic Si-detector arrays affected by optical crosstalk," *IEEE Trans. Electron. Dev.* **ED-27**(1), 189–193 (1980).
4. S. G. Chamberlain and D. H. Harper, "MTF simulation including transmittance effects of CCD," *IEEE Trans. Electron. Dev.* **ED-25**(2), 145–154 (1978).
5. J. P. Lavine, E. A. Trabka, B. C. Burkey, T. J. Tredwell, E. T. Nelson, and C. N. Anagnostopoulos, "Steady-state photocarrier collection in silicon imaging devices," *IEEE Trans. Electron. Dev.* **ED-30**(9), 1123–1134 (1983).
6. J. P. Lavine, W. Chang, C. N. Anagnostopoulos, B. C. Burkey, and E. T. Nelson, "Monte Carlo simulation of the photoelectron crosstalk imaging devices," *IEEE Trans. Electron. Dev.* **ED-32**(10), 2087–2091 (1985).
7. D. Levy, S. E. Schacham, and I. Kidron, "Three-Dimensional analytical simulation of self cross-responsitivities of photovoltaic detector arrays," *IEEE Trans. Electron. Dev.* **ED-34**(10), 2059–2070 (1987).
8. E. G. Stevens and J. P. Lavine, "An analytical, aperture, and two-layer carrier diffusion MTF and quantum efficiency model for solid-state image sensors," *IEEE Trans. Electron. Dev.* **41**(10), 1753–1760 (1994).
9. P. R. Jorden, J. Deltorn, and A. P. Oates, "The non-uniformity of CCD's and the effects of spatial undersampling," *Proc. SPIE* **2198**, 836–850 (1994).
10. S. K. Mendis, S. E. Kemeny, R. C. Gee, B. Pain, Q. Kim, and E. F. Fossum, "Progress in CMOS active pixel sensors," *Proc. SPIE* **2172**, 19–29 (1994).
11. G. Wan, X. Gong, Z. Luo, and F. Jing, "Studies on the measurements of CTE and photoresponse nonuniformity of linear CCD's," *Opt. Eng.* **34**(11), 3254–3260 (1995).
12. W. Wittenstein, J. C. Fontanella, A. R. Newbery, and J. Baars, "The definition of OTF and the measurement of aliasing for sampled imaging systems," *Opt. Acta* **29**(1), 41–50 (1982).
13. S. K. Park, R. Schowengerdt, and M. A. Kaczynski, "MTF analysis for sampled image systems," *Appl. Opt.* **23**(15), 2572–2582 (1984).
14. L. de Luca and G. Gardone, "Modulation transfer function cascade model for a sampled IR imaging system," *Appl. Opt.* **30**(13), 1659–1664 (1991).
15. A. H. Lettington and Q. H. Hong, "Measurement of the discrete modulation transfer function," *J. Mod. Opt.* **40**(2), 203–212 (1993).
16. M. Corba, Z. Ninkov, B. S. Backer, M. Wu, and B. Slawson, "Preliminary results with a CID based photon counting system," *Proc. SPIE* **2654**, 310–316 (1996).
17. J. A. Holtzman, "The performance and calibration of WFPC2Telescope," *Publ. Astron. Soc. Pac.* **107**(708), 156–178 (1995).
18. L. B. Robinson, M. Z. Wei, W. J. Borucki, E. W. Dunham, C. H. Ford, and A. F. Granados, "Test of CCD precision limits for differential photometry," *Publ. Astron. Soc. Pac.* **107**(717), 1094–1098 (1995).
19. R. Toledo-Crow, P. C. Yang, Y. Chen, and M. Vaez-Iravani, "Near-field differential scanning optical microscope with atomic force regulation," *Appl. Phys. Lett.* **60**(24), 2957–2959 (1992).
20. M. Born and E. Wolf, *Principles of Optics*, Wiley, New York (1967).
21. B. F. Alexander and K. C. Ng, "Elimination of systematic error in subpixel estimation," *Opt. Eng.* **30**(9), 1320–1330 (1991).
22. J. P. Fillard, H. M'timet, J. M. Lussert, and M. Castagne, "Computer simulaton of super-resolution point source image detection," *Opt. Eng.* **32**(11), 2936–2944 (1993).

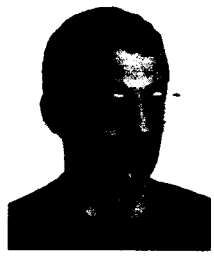

Daniel Kavaldjiev received his BS and MS degrees in applied physics from Sofia University, Bulgaria. He is currently working toward his PhD in imaging science in the Center for Imaging Science at the Rochester Institute of Technology. His research interests include optical microscopy, optical metrology and solid state light detector characterization.

Zoran Ninkov completed his BSc (with first class honors) in physics at the University of Western Australia, his MSc in physical chemistry at Monash University and his PhD in astronomy at the University of British Columbia. He is currently an associate professor in the Center for Imaging Science at the Rochester Institute of Technology. His research interests are in the development of new solid state focal plane array sensors, the evaluation of such devices, the use of these devices in astronomical and other remote sensing applications, and the development of multiobject spectroscopy techniques.